Supplementary Information

Clearance of senescent cells by ABT263 rejuvenates aging hematopoietic stem cells in mice

Jianhui Chang, Yingying Wang, Lijian Shao, Remi–Martin Laberge, Marco Demaria, Judith Campisi, Krishnamurthy Janakiraman, Norman E. Sharpless, Sheng Ding, Wei Feng, Yi Luo, Xiaoyan Wang, Nukhet Aykin–Burns, Kimberly Krager, Usha Ponnappan, Martin Hauer–Jensen, Aimin Meng, and Daohong Zhou

Supplementary Item & Number	**Title**
Supplementary Figure 1	Analysis of WI–38 cell senescence and effect of ABT263 on the viability of IR–induced senescent WI–38 cells in culture
Supplementary Figure 2	TBI induces SC accumulation in p16–3MR mice in a time dependent manner
Supplementary Figure 3	Mechanism of action of ABT263
Supplementary Figure 4	TBI induces HSC senescence in mice
Supplementary Figure 5	Clearance of SCs by ABT263 does not reduce BM HSCs and HPCs in TBI mice
Supplementary Figure 6	Clearance of SCs by ABT263 improves the engraftment ability of HSCs from TBI mice in secondary BMT recipients
Supplementary Figure 7	Clearance of SCs by ABT263 attenuates TBI–induced disruption of HSC quiescence and sustained DNA damage in HSCs
Supplementary Figure 8	Clearance of SCs by ABT263 promotes B cell lymphopoiesis in TBI mice
Supplementary Figure 9	ABT263 selectively eliminates TBI–induced senescent HSCs in culture and abrogates TBI-induced SASP in BM HSCs and bone stromal cells

Nature Medicine: doi:10.1038/nm.4010

Supplementary Figure 10	Clearance of SCs by ABT263 improves the clonogenic activity and engraftment ability of HSCs from normally aged mice
Supplementary Figure 11	ABT263 reduces senescent MuSCs in normally aged mice
Supplementary Table 1	EC_{50} for various compounds against non-senescent and IR–induced senescent WI–38 cells
Supplementary Table 2	Suppliers for various compounds and cytokines
Supplementary Table 3	Antibodies for western blot analyses
Supplementary Table 4	Antibodies for flow cytometry and cell sorting
Supplementary Table 5	Sequences of the primers used for qRT–PCR

Nature Medicine: doi:10.1038/nm.4010

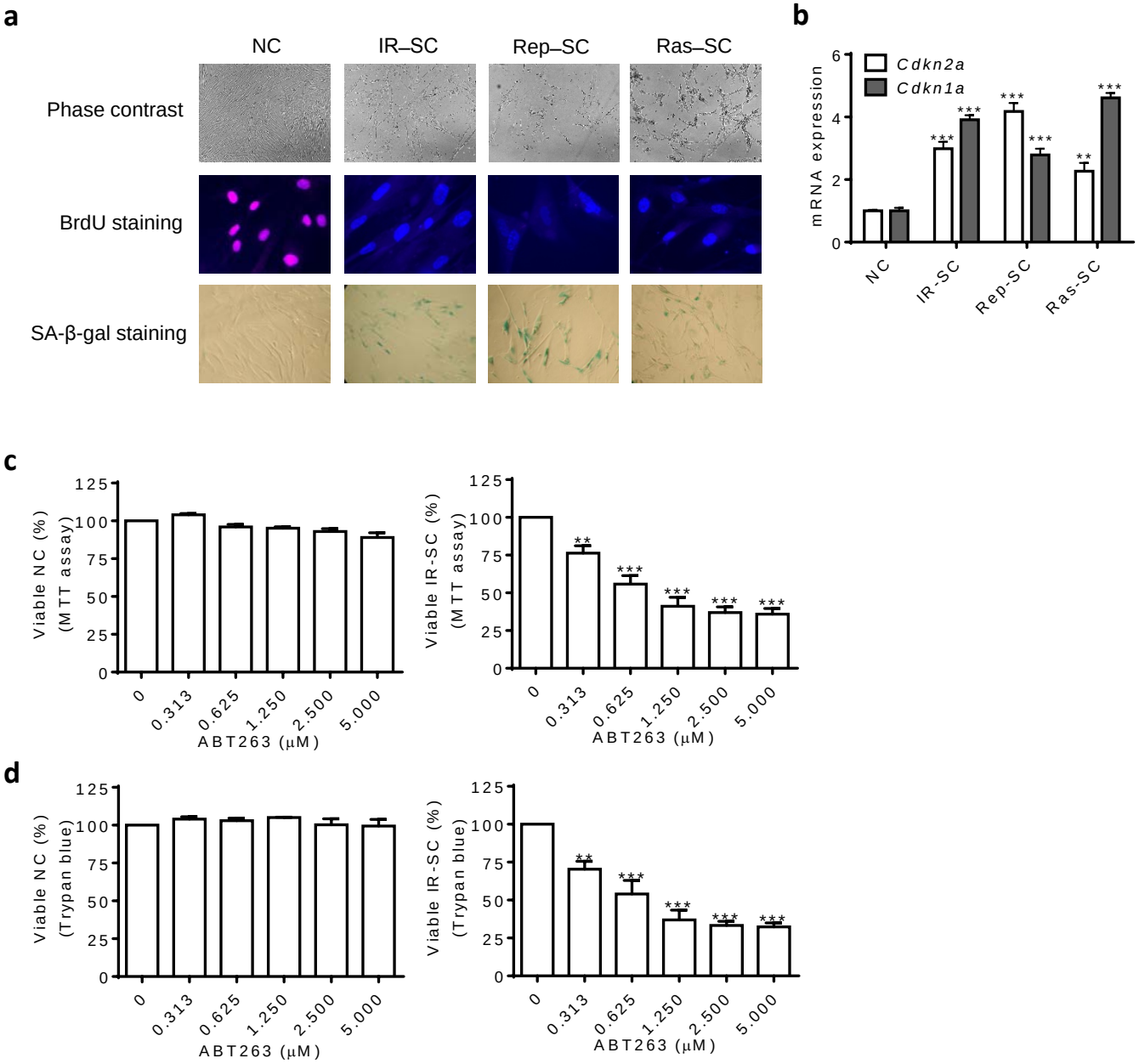

e

EC_{50} values of ABT263

Cell types	EC_{50} (μM)	EC_{50} Ratio (NC / SC)
NC	12.60	–
IR-SC	0.61	20.66
Rep-SC	1.45	8.69
Ras-SC	0.62	20.32

Supplementary Figure 1 Analysis of WI–38 cell senescence and effect of ABT263 on the viability of IR–induced senescent WI–38 cells in culture. (**a**) Representative phase contrast, BrdU staining and SA–β–gal staining micrographs of non–senescent (NC) and senescent WI–38 cells induced by IR (IR–SC), replicative exhaustion (Rep–SC) or expression of oncogenic Ras (Ras–SC). (**b**) IR–SC, Rep–SC and Ras–SC express increased levels of *Cdkn2a* and *Cdkn1a* mRNA compared to NC. The data are presented as means ± s.e.m. of fold changes from 3 independent experiments. $^{**}P < 0.01$ and $^{***}P < 0.001$ vs. NC by unpaired t test. (**c**) MTT assay and (**d**) trypan blue exclusion test confirm that ABT263 dose–dependently kills senescent WI–38 fibroblasts (WI38) induced by ionizing radiation (IR–SC), but is not cytotoxic to non–senescent WI–38 cells (NC). Viable cells were quantified after treating with increasing concentrations of ABT263 for 72 h. The data presented are means ± s.e.m. of viable cells as a percent of control without ABT263 treatment from 3 or more independent experiments. $^{**}P < 0.01$ and $^{***}P < 0.001$, vs. without ABT263 by one–way ANOVA. (**e**) EC_{50} values of ABT263 against NC and SC.

Nature Medicine: doi:10.1038/nm.4010

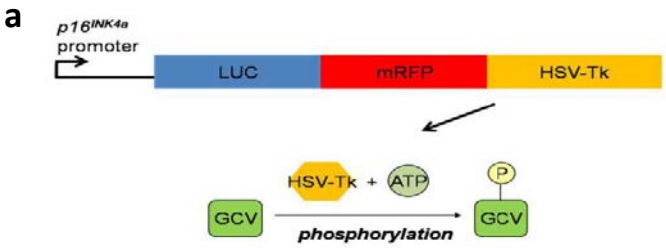

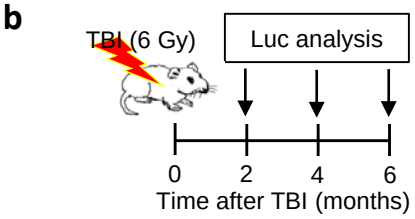

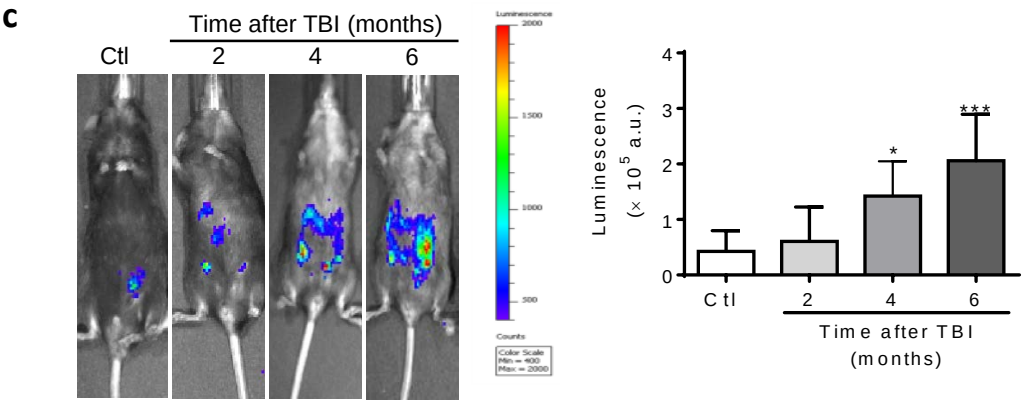

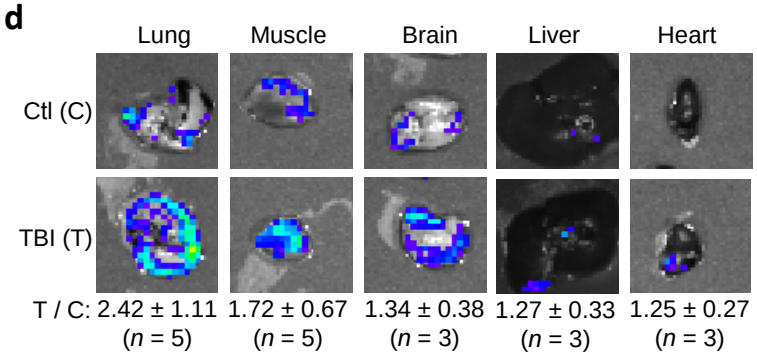

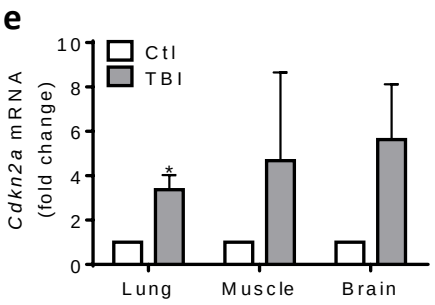

Nature Medicine: doi:10.1038/nm.4010

Supplementary Figure 2

Supplementary Figure 2 TBI induces SC accumulation in p16–3MR mice in a time dependent manner. (**a**) A diagram depicting the p16–3MR transgene. (**b**) A diagram illustrating the experimental design. Specifically, male p16–3MR mice were exposed to a sublethal dose (6 Gy) of TBI at 2 months of age. Before (Ctl) and 2, 4, and 6 months after TBI, whole body luminescence was quantified. The mice were euthanized the day after the last imaging to harvest tissues for luminescence quantification and analysis of *Cdkn2a* mRNA levels by qRT–PCR. (**c**) Whole body luminescence imaging shows that TBI induces SC accumulation in p16–3MR mice in a time dependent manner. Left panel: representative luminescent images of control (Ctl) and TBI p16–3MR mice (TBI); and right panel: whole body luminescence quantification. (**d**) Representative luminescent images of the lungs, skeletal muscle, brain, liver and heart from control (Ctl) and TBI p16–3MR mice. The numbers below the images are means ± s.e.m. of fold changes of luminescence in various tissues compared to that of Ctl. (**e**) Analysis of *Cdkn2a* mRNA levels in the lungs, skeletal muscle, and brain confirms that TBI increases SCs in these tissues. The data are presented as means ± s.e.m. of fold changes from Ctl (n = 3 mice/group). *P < 0.05 vs. Ctl. One–way ANOVA for **c** and unpaired t test for **e**.

Nature Medicine: doi:10.1038/nm.4010

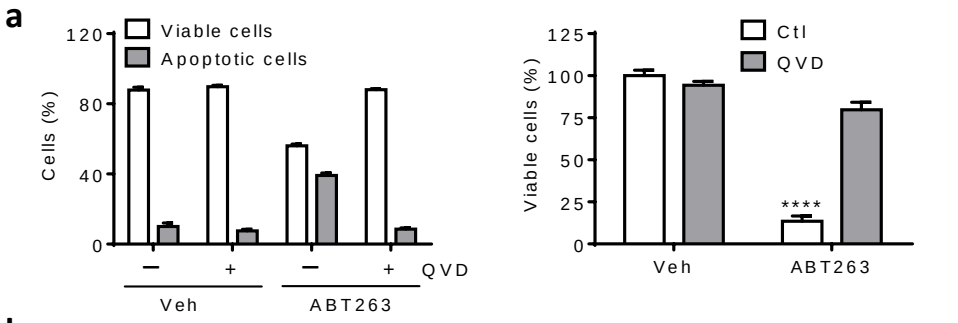

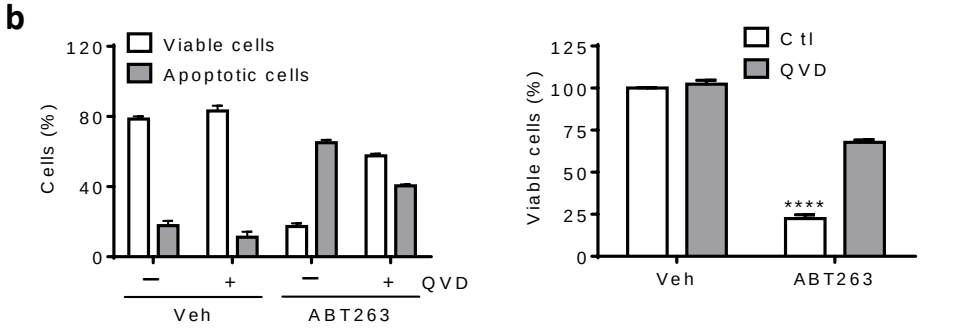

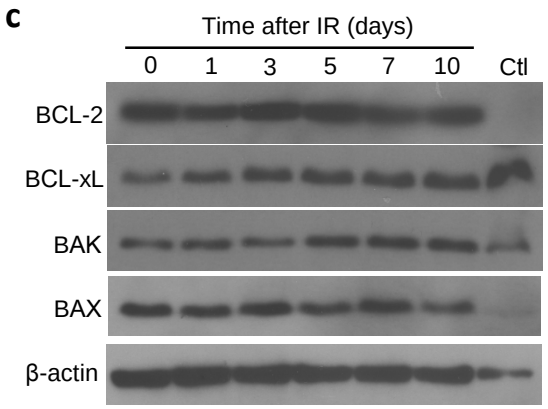

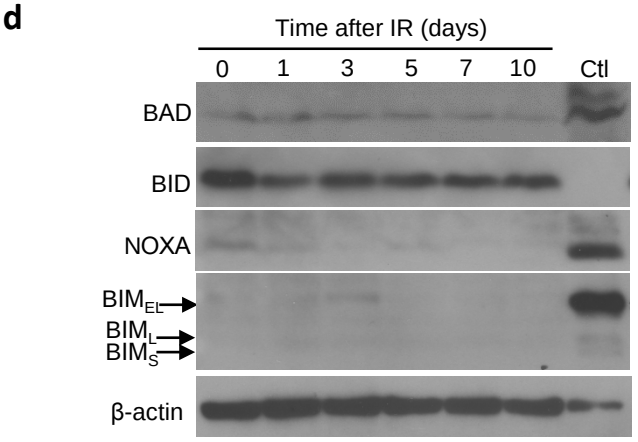

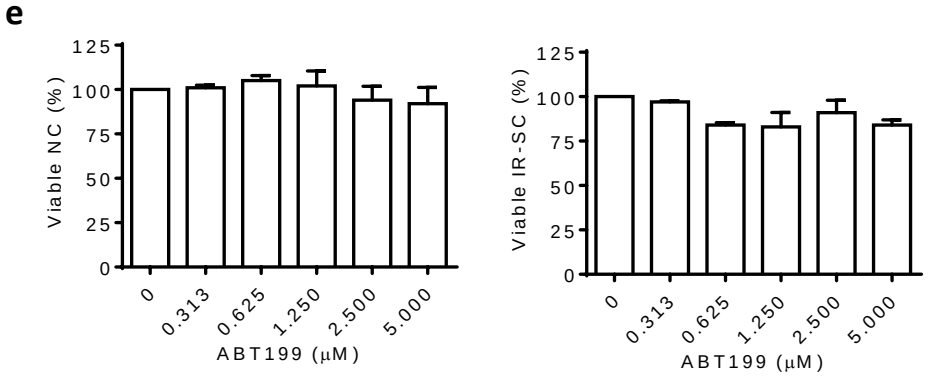

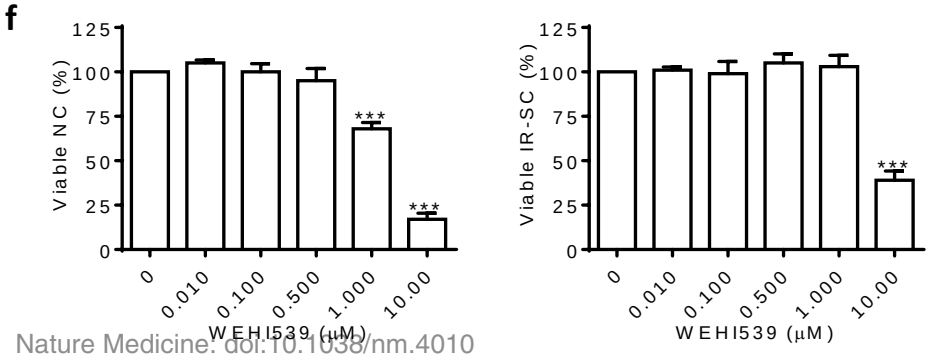

Nature Medicine: doi:10.1038/nm.4010

Supplementary Figure 3

Supplementary Figure 3 Mechanism of action of ABT263. (**a & b**) ABT263 induces apoptosis in IR–induced senescent IMR–90 fibroblasts (**a**) and human renal epithelial cells (**b**) in a caspase–dependent manner as shown in **Fig. 2a** for WI-38 cells. Left panel: percentages of viable cells (PI^-Annexin V^- cells) and apoptotic cells (PI^-Annexin V^+ cells + PI^+Annexin V^+ cells) 24 h after treatment with vehicle or ABT263 ± QVD. Right panel: Quantification of the percentage of viable IR-SC 72 h after treatment with vehicle or ABT263 ± QVD. The data are presented as means ± s.e.m. of 3 independent experiments. ****$P < 0.0001$ vs. Ctl by two–way ANOVA. (**c & d**) A representative western blot of BCL–2, BCL–xL, BAK and BAX in WI–38 cells at various times after exposure to 10 Gy IR is shown in **c** and that of BAD, BID, NOXA, and BIM in **d**. β–actin is used as a loading control. Ctl represents a positive control using cell lysates from K562 cells treated with 2 μM MG132 for 24 h. (**e & f**) Inhibition of Bcl–2 or Bcl–xL alone does not selectively kill senescent WI–38 cells. (**e**) ABT199 (a specific Bcl–2 inhibitor) is not cytotoxic to senescent WI–38 cells induced by ionizing radiation (IR–SC) or non–senescent WI–38 cells (NC). (**f**) WEHI539 (a specific Bcl–xL inhibitor) does not selectively kill IR–SC. Viable cells were quantified after treatment with increasing concentrations of ABT199 or WEHI593 for 72 h. The data presented are means ± s.e.m. of viable cells as a percent of control without ABT199 or WEHI593 treatment from 3 independent experiments. ***$P < 0.001$ vs. without ABT199 or WEHI593 by one–way ANOVA.

Nature Medicine: doi:10.1038/nm.4010

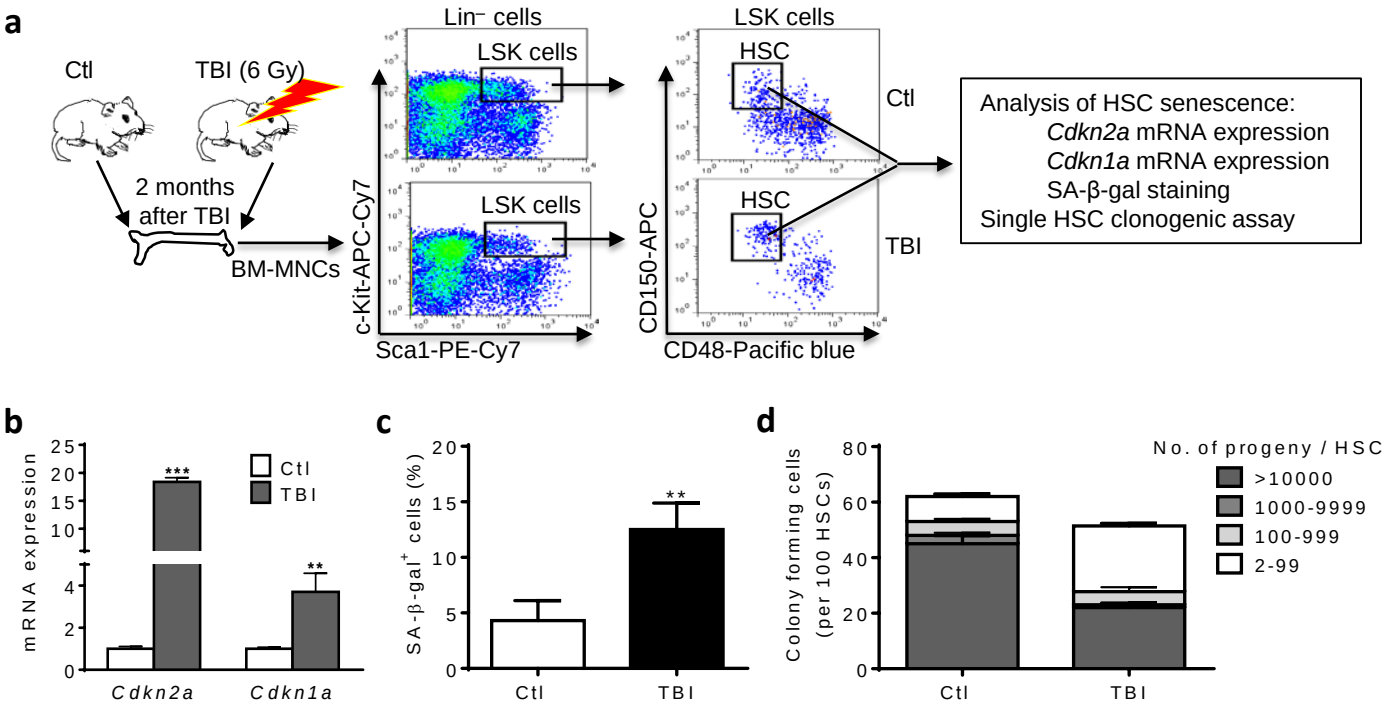
a
Ctl
TBI (6 Gy)
2 months
after TBI
BM-MNCs
Lin⁻ cells
LSK cells
LSK cells
c-Kit-APC-Cy7
Sca1-PE-Cy7
LSK cells
HSC
Ctl
HSC
TBI
CD150-APC
CD48-Pacific blue
Analysis of HSC senescence:
Cdkn2a mRNA expression
Cdkn1a mRNA expression
SA-β-gal staining
Single HSC clonogenic assay

b
mRNA expression
Ctl
TBI
***
**
Cdkn2a
Cdkn1a
c
SA-β-gal+ cells (%)
**
Ctl
TBI
d
Colony forming cells
(per 100 HSCs)
No. of progeny / HSC
>10000
1000-9999
100-999
2-99
Ctl
TBI

Supplementary Figure 4 TBI induces HSC senescence in mice. (**a**) A diagram illustrating the strategy to isolate mouse bone marrow (BM) HSCs ($CD150^{+}CD48^{-}LSK$ cells) from control non-irradiated mice (Ctl) and sublethally total body irradiated (TBI) mice for analysis of HSC senescence and single HSC clonogenic activity. (**b** & **c**) HSCs from TBI mice express higher levels of *Cdkn2a* and *Cdkn1a* mRNA and SA–β–gal activity than cells from control non-irradiated mice (Ctl). The data are presented as means ± s.e.m. of fold changes from 3 independent experiments for **b** and means ± s.e.m. of percent of $SA–β–gal^{+}$ cells from 4 Ctl mice and 3 TBI mice for **c**. $^{**}P < 0.01$ and $^{***}P < 0.001$ vs. Ctl by unpaired t test. (**d**) Clonogenic activity was determined after individual BM HSCs were cultured at 1 cell/well in HSC expansion medium for 14 d. The data presented in **c** are means ± s.e.m. of percent of single HSCs having the ability to produce different nubmers of progeny ($n = 2$ independent experiments with pooled HSCs from 3–4 mice per group).

Nature Medicine: doi:10.1038/nm.4010

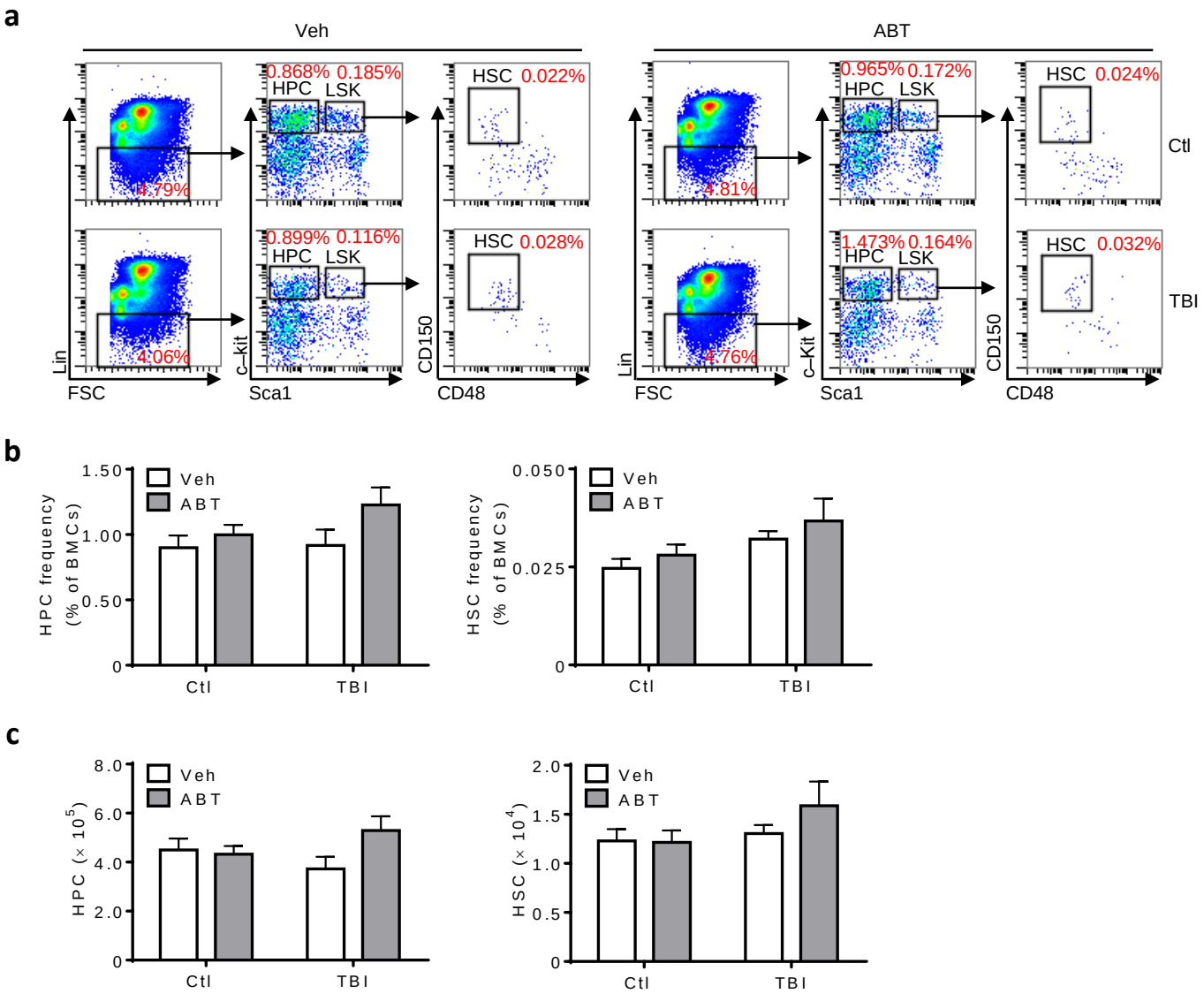
a
Veh
ABT
0.868% 0.185%
HPC LSK
HSC 0.022%
4.79%
0.899% 0.116%
HPC LSK
HSC 0.028%
4.06%
0.965% 0.172%
HPC LSK
HSC 0.024%
4.81%
1.473% 0.164%
HPC LSK
HSC 0.032%
4.76%
Ctl
TBI
Lin
FSC
c–kit
Sca1
CD150
CD48
c–Kit
b
HPC frequency (% of BMCs)
HSC frequency (% of BMCs)
Veh
ABT
Ctl
TBI
c
HPC (× 10^5)
HSC (× 10^4)

Supplementary Figure 5 Clearance of SCs by ABT263 does not reduce BM HSCs and HPCs in TBI mice. (**a**) Representative flow cytometric analyses of HSCs and HPCs ($Lin^{-}Sca1^{-}$ $c–kit^{+}$ cells) in BM cells (BMCs) from control (Ctl) or TBI mice after treatment with vehicle (Veh) or ABT263 (ABT) as shown in **Fig. 3a**. (**b**) The frequencies of HPCs and HSCs in BMCs. (**c**) The numbers of HPCs and HSCs in the hind legs from each mouse. The data are presented as means ± s.e.m. (n = 8 – 11 mice per group).

Nature Medicine: doi:10.1038/nm.4010

a

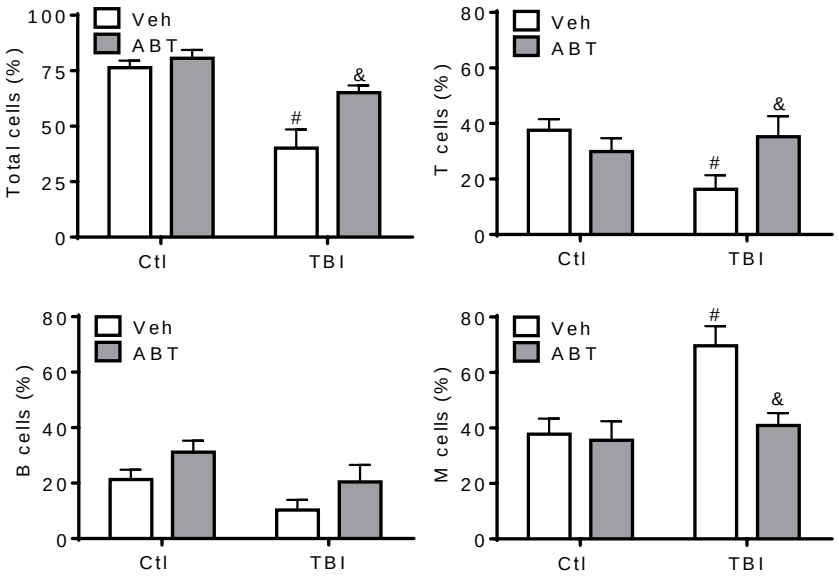

Supplementary Figure 6

Supplementary Figure 6 Clearance of SCs by ABT263 improves the engraftment ability of HSCs from TBI mice in secondary BM transplantation (BMT) recipients. BMT was done as shown in **Fig. 3d**. The engraftment of donor–derived total white blood cells ($CD45.2^+$), T cells ($CD45.2^+Thy–1.2^+$), B cells ($CD45.2^+B220^+$), and myeloid cells (M cells, $CD45.2^+CD11b/Gr–1^+$) in secondary recipient peripheral blood is shown. The data are presented as means ± s.e.m.(*n* = 6 recipients per group). $^{\#}P < 0.05$ vs. Ctl and $^{\&}P < 0.05$ vs. TBI + Veh by two–way ANOVA.

Nature Medicine: doi:10.1038/nm.4010

a

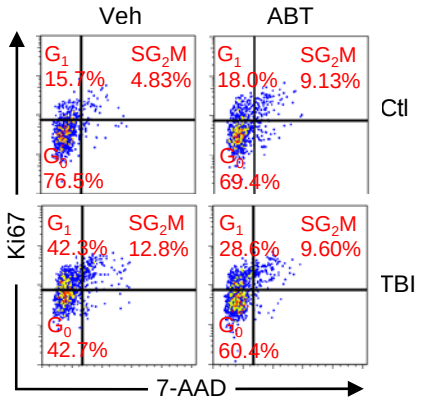
Veh
ABT
G1
15.7%
SG2M
4.83%
G0
76.5%
G1
18.0%
SG2M
9.13%
G0
69.4%
Ctl
Ki67
G1
42.3%
SG2M
12.8%
G0
42.7%
G1
28.6%
SG2M
9.60%
G0
60.4%
TBI
7-AAD

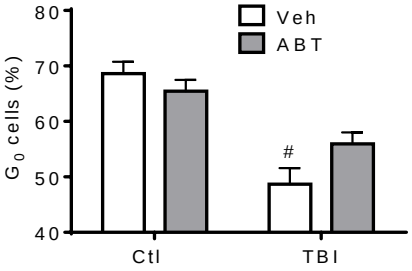
80
70
60
50
40
G0 cells (%)
Veh
ABT
#
Ctl
TBI

b

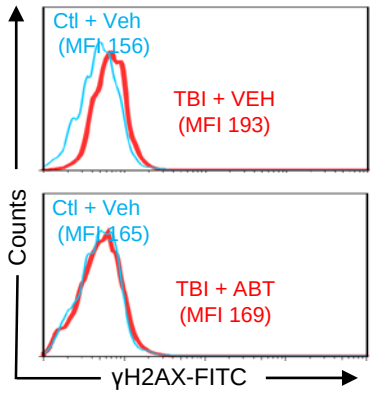
Ctl + Veh
(MFI 156)
TBI + VEH
(MFI 193)
Ctl + Veh
(MFI 165)
TBI + ABT
(MFI 169)
Counts
γH2AX-FITC

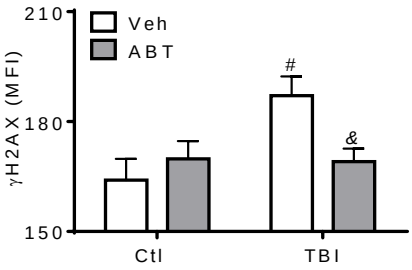
210
180
150
γH2AX (MFI)
Veh
ABT
#
&
Ctl
TBI

Supplementary Figure 7 Clearance of SCs by ABT263 attenuates TBI–induced disruption of HSC quiescence and sustained DNA damage in HSCs. (**a**) Left panel, representative flow cytometric analyses of the cell cycle distribution of HSCs from control (Ctl) or TBI mice after treatment with vehicle (Veh) or ABT263 (ABT). Right panel, the percentages of G_0 cells in HSCs ($Ki67^-$ cells). (**b**) Left panel, representative flow cytometric analyses of γH2AX staining to detect DNA double strand breaks in HSCs from control (Ctl) or TBI mice after treatment with vehicle (Veh) or ABT263 (ABT). Right panel, the mean fluorescence intensity (MFI) of γH2AX staining in HSCs. The data are presented as means ± s.e.m. (n = 8 – 11 mice per group for **a** and 5–11 mice per group for **b**). $^{\#}P < 0.05$ vs. Ctl and $^{\&}P < 0.05$ vs. TBI + Veh by two–way ANOVA.

Nature Medicine: doi:10.1038/nm.4010

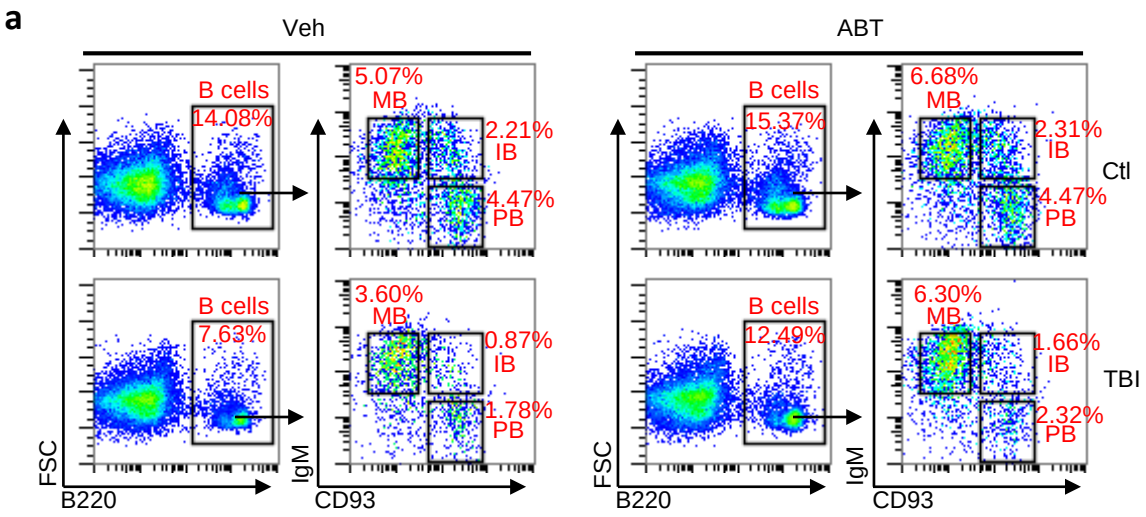
a
Veh
ABT
B cells
14.08%
5.07%
MB
2.21%
IB
4.47%
PB
B cells
7.63%
3.60%
MB
0.87%
IB
1.78%
PB
B cells
15.37%
6.68%
MB
2.31%
IB
4.47%
PB
Ctl
B cells
12.49%
6.30%
MB
1.66%
IB
2.32%
PB
TBI
FSC
B220
IgM
CD93

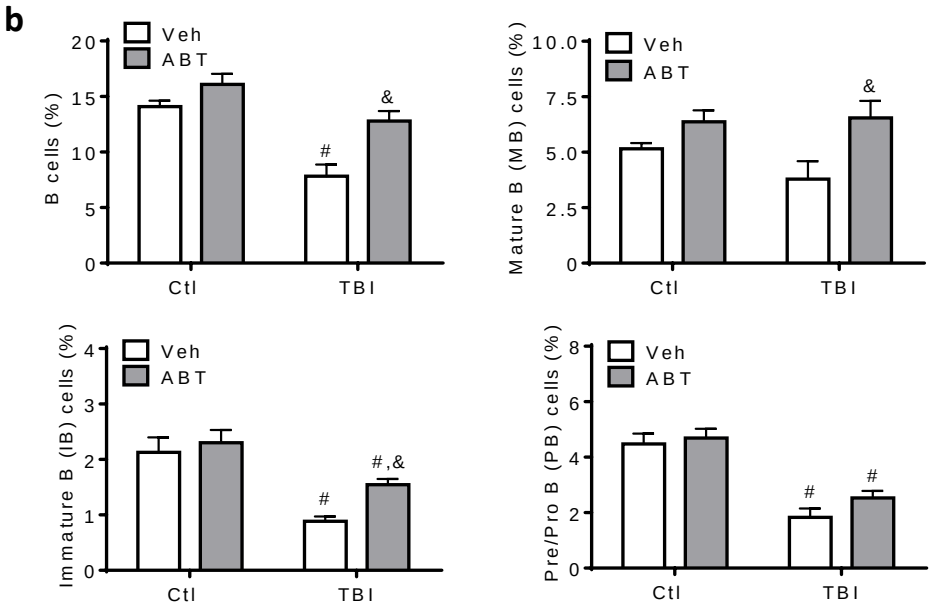
b
Veh
ABT
B cells (%)
Ctl
TBI
Mature B (MB) cells (%)
Immature B (IB) cells (%)
Pre/Pro B (PB) cells (%)

Supplementary Figure 8 Clearance of SCs by ABT263 promotes B cell lymphopoiesis in TBI mice. (**a**) Representative flow cytometric analyses of B cells ($B220^+$), mature B cells (MB, $B220^+IgM^+CD93^-$), immature B cells (IB, $B220^+IgM^+CD93^+$), and Pre/Pro–B cells (PB, $B220^+IgM^-CD93^+$) in BMCs from control (Ctl) or TBI mice after treatment with vehicle (Veh) or ABT263 (ABT) as shown in **Fig. 3a**. (**b**) The frequencies of B cells, mature B cells, immature B cells, and Pre–Pro–B cells in BMCs are presented as means ± s.e.m. (n = 4 – 6 mice per group). $^{\#}P < 0.05$ vs. Ctl and $^{\&}P < 0.05$ vs. TBI + Veh by two–way ANOVA.

Nature Medicine: doi:10.1038/nm.4010

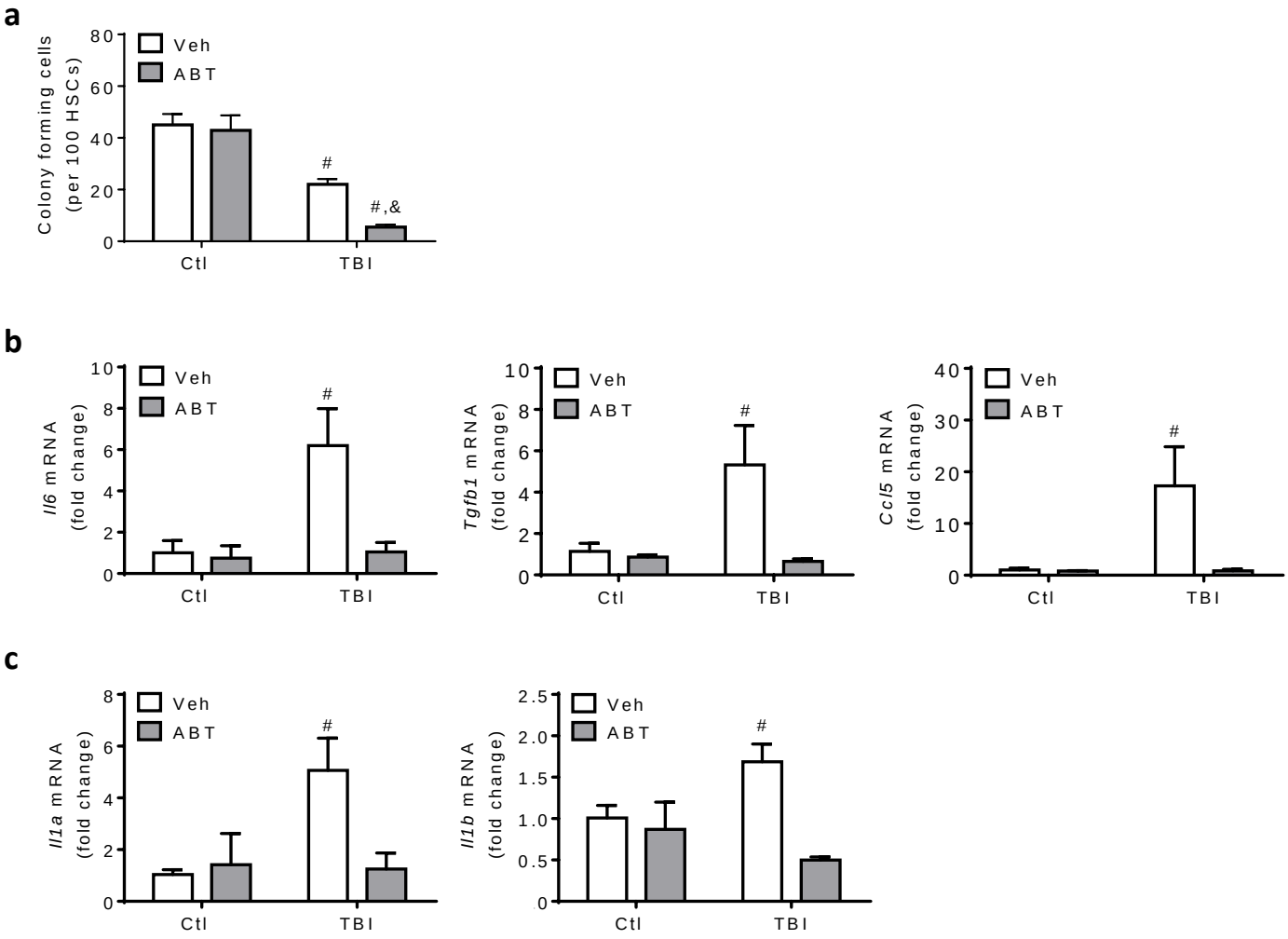

Supplementary Figure 9

Supplementary Figure 9 ABT263 selectively eliminates TBI–induced senescent HSCs in culture and abrogates TBI-induced SASP in BM HSCs and bone stromal cells. (**a**) ABT263 selectively eliminates TBI-induced senescent HSCs in culture. Colony forming activity of single HSCs isolated from control non-irradiated mice (Ctl) or mice 2 months after exposure to 6 Gy TBI was analyzed in the presence of vehicle (Veh) or ABT263 (ABT, 1.25 μM). The data are presented as means ± s.e.m (*n* = 3 independent assays) of HSCs that were capable of producing more than 10,000 progeny. (**b** and **c**) ABT263 inhibits TBI-induced SASP in HSCs and bone stromal cells. BM HSCs and bone stromal cells were isolated from control non-irradiated mice (Ctl) or TBI mice treated with vehicle (Veh) or ABT263 (ABT) as shown in **Fig. 3a** and analyzed for SASP mRNA levels by qPCR. (**b**) Levels of *Il6*, *Tgfb1* and *Ccl5* mRNAs in HSCs. (**c**) Levels of *Il1a* and *Il1b* mRNAs in bone stromal cells. Levels of *Il1a*, *Il1b*, *Tnfa*, and *Cxcl10* mRNA in HSCs and those of *Il6*, *Tgfb1*, *Tnfa*, *Ccl5* and *Cxcl10* mRNA in bone stromal cells were not elevated by TBI (data not shown). The data presented in **b** and **c** are means ± s.e.m. of fold changes from vehicle-treated control mice. *n* = 3 mice/group for Ctl and 5 mice/group for TBI. $^{\#}P < 0.05$ vs. Ctl and $^{\&}P < 0.05$ vs. TBI + Veh by two–way ANOVA.

Nature Medicine: doi:10.1038/nm.4010

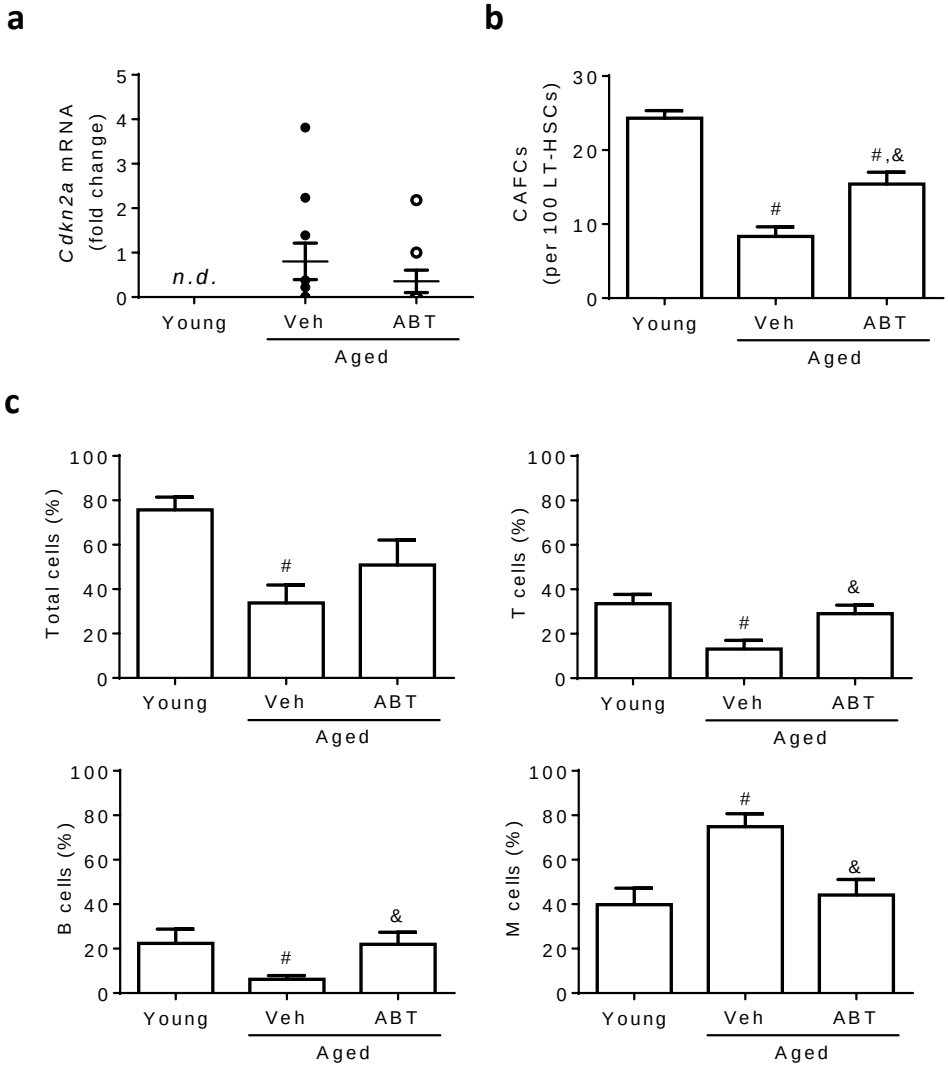

Supplementary Figure 10

Supplementary Figure 10 Clearance of SCs by ABT263 improves the clonogenic activity and engraftment ability of HSCs from normally aged mice. (**a**) The expression of *Cdkn2a* mRNA in BM HSCs was analyzed by qPCR and presented as fold changes from aged mice treated with vehicle. *n.d.*, not detectable. n = 9, 10, and 11 mice/group for Young, Aged + Veh, and Aged + ABT, respectively. (**b**) Single HSC CAFC assay shows that ABT263 improves clonogenic function of HSCs from aged mice. n = 7, 11, and 10 mice/group for Young, Aged + Veh, and Aged + ABT, respectively. (**c**) Engraftment of donor–derived total white blood cells ($CD45.2^+$), T cells ($CD45.2^+Thy–1.2^+$), B cells ($CD45.2^+B220^+$), and myeloid cells (M cells, $CD45.2^+CD11b/Gr–1^+$) in secondary recipients' peripheral blood is shown. The data are presented as means ± s.e.m. (n = 6, 10, and 6 recipients per group for Young, Aged + Veh, and Aged + ABT, respectively). $^{\#}P < 0.05$ vs. Young and $^{\&}P < 0.05$ vs. Aged + Veh by two–way ANOVA.

Nature Medicine: doi:10.1038/nm.4010

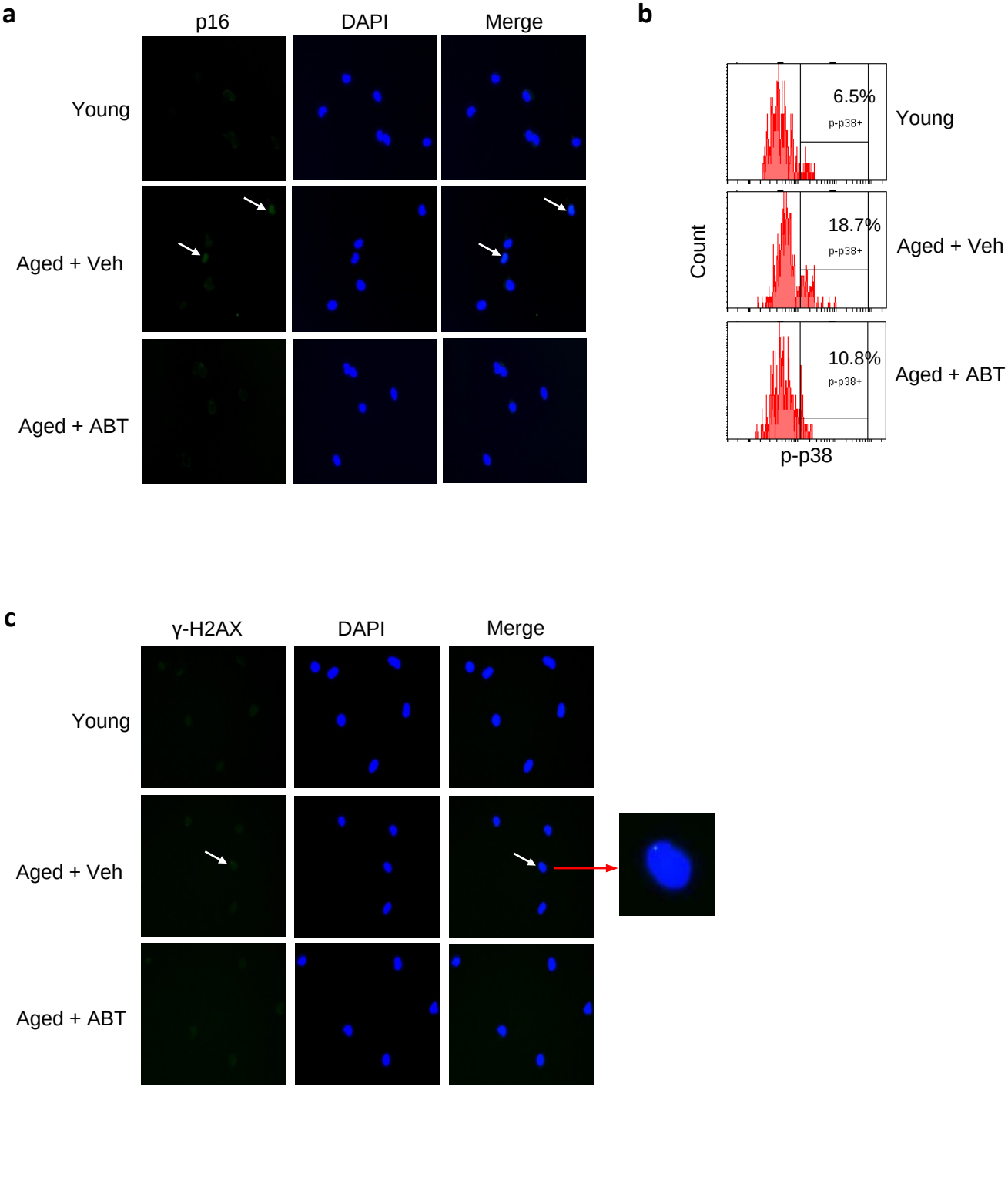

Supplementary Figure 11

Supplementary Figure 11. ABT263 reduces senescent MuSCs in normally aged mice. (**a**) Representative micrograph of p16 immunostaining of sorted MuSCs from young and aged mice treated with vehicle (Veh) or ABT263 (ABT). White arrows indicate $p16^{+}$ senescent MuSCs. (**b**) Representative flow cytometric analysis of phosphorylated p38 (p-p38) immunostaining in MuSCs from young and aged mice treated with vehicle (Veh) or ABT263 (ABT). (**c**) Representative micrograph images of γH2AX immunostaining of the sorted MuSCs from young and aged mice treated with vehicle (Veh) or ABT263 (ABT). White arrows indicate a MuSC with a γH2AX focus.

Nature Medicine: doi:10.1038/nm.4010

Supplementary Table 1. EC_{50} for compounds administered to non–senescent WI–38 cells (NC) and IR–induced senescent WI–38 cells (SC)

Compound name	Mechanism(s) of action	EC_{50} (μM), non–senescent cells (NC)	EC_{50} (μM), senescent cells (SC)	EC_{50} Ratio (NC/SC)
ABT263	Bcl–2, Bcl–xL, Bcl–w inhibitor	12.60	0.61	20.6
ABT199	Bcl–2 inhibitor	> 10.00	> 10.00	1.0
WEHI539	Bcl–xL inhibitor	2.80	3.88	0.7
MIM1	Mcl–1 inhibitor	> 50.00	> 50.00	1.0
2–Deoxy–D–glucose	Glycolysis inhibitor	4800.00	8890.00	0.5
3–Bromopyruvate	Glycolysis and TCA inhibitor	280.00	370.00	0.8
Auranofin	TrxR inhibitor	5.13	5.34	1.0
Buthionine sulfoximine	γ–GSC inhibitor	2340.19	2391.51	1.0
Decyl–triphenylphosphonium	ROS inducer	1.41	0.98	1.4
Arsenic trioxide	ROS inducer	15.65	18.26	0.9
Dehydroepiandrosterone	PPP inhibitor	296.20	509.51	0.6
Rapamycin[a]	mTOR inhibitor	> 0.04	> 0.04	1.0
Metformin[a]	AMPK activator	> 20,000	> 20,000	1.0
Psychosine	Lysosome toxin	46.32	52.25	0.9
Balifomycin A1	(V)–ATPase inhibitor	29.71	22.11	1.3
Despramine	ASM inhibitor	50.03	51.13	1.0
Terfenadine	ASM inhibitor	6.13	6.87	0.9
Nutlin3[b]	Mdm2 inhibitor	5.62	82.16	0.1
KU55933	ATM inhibitor	5.10	30.73	0.2
NU7026	DNA–PK inhibitor	47.02	64.03	0.7
SB202190[c]	p38 MAPK inhibitor	> 800.00	> 800.00	1.0
Parthenolide[d]	NF–κB inhibitor	11.46	12.57	0.9
BMS345541[d]	IKKβ inhibitor	6.87	10.79	0.6
JQ1	BRDT / c–Myc inhibitor	0.12	1.93	0.1
MG132	Proteasome inhibitor	0.24	1.92	0.1
IPI–504	HSP 90 inhibitor	0.14	0.93	0.2

Nature Medicine: doi:10.1038/nm.4010

Echinomycin	HIF1α inhibitor	0.42	2.86	0.2
CPI–613	PDH and α–ketoglutarate dehydrogenase inhibitor	222.92	205.20	1.1
Plumbagin	Anti–cancer agent, ROS producer	12.63	8.70	1.5
Bortzomib	26S proteasome inhibitor	0.016	0.024	0.7
Wogonin	Anti–cancer agent, ROS producer	> 200.00	> 200.00	1.0
Phenethyl isothiocyanate (PEITC)	ROS producer, Akt inactivator, JNK activator	< 10.00	> 10.00	< 1.0
Spermine	Polyamine	> 40.00	> 40.00	1.0
YM–155	Survivin inhibitor	78.43	50.02	1.6
Hydrogen peroxide	ROS	134.80	230.70	0.58
Trichostatin A (TSA)	HDAC inhibitor	0.72	0.39	1.87
Vorinostat (SAHA)	HDAC inhibitor	0.85	2.21	0.38

AMPK: AMP–activated protein kinase; ASM: Acid sphingomyelinase; ATM: Ataxia telangiectasia mutated; BRDT: Bromodomain testis–specific protein; DNA–PK: DNA–dependent protein kinase; γ–GSC: γ–glutamylcysteine synthetase; HDAC: Histone deacetylase; HIF1α: hypoxia inducible factor 1α; HSP 90: Heat–shock protein 90; IKKβ: IκB kinase β; JNK: Jun N–terminal kinase; MAPK: Mitogen–activated protein kinase; PDH: Pyruvate dehydrogenase; PPP: Pentose phosphate pathway; TCA: Citric acid cycle; TrxR: Thioredoxin reductase;

Footnotes:

[a]Rapamycine and metformin can inhibit the mTOR pathway directly and indirectly via activation of the LKB1/AMPK pathway, respectively. The mTOR pathway is important in regulation of cellular senescence (Blagosklonny MV. Drug Discov Today. 2007;12:218–24).

[b]Nutlin3 promotes the induction of cellular senescence by activating the p53 pathway (Schug TT. Aging (Albany NY). 2009;1:842–4).

[c]SB202190 inhibits the p38 pathway that is important for the induction of cellular senescence (Xu Y et al. Trends Biochem Sci. 2014;39:268–76).

[d]Both parthenolide and BMS345541 inhibit the IKK–NFκB pathway and NFκB inhibition can delay DNA–damage–induced senescence (Tilstra JS et al. J Clin Invest. 2012;122:2601–12).

Nature Medicine: doi:10.1038/nm.4010

Supplementary Table 2. Suppliers for compounds and cytokines

Compound name	Suppliers	Catalog #
ABT263	Selleckchem, Houston, TX,USA	S1001
ABT199	Selleckchem, Houston, TX,USA	S8048
WEHI539	APExBIO , Houston, TX,USA	A3935
MIM1	APExBIO, Houston, TX,USA	A4465
2–Deoxy–D–glucose	provided by Dr. Arkin–Burns*	
3–bromopyruvate	Sigma, St. Louis, MO, USA	16490
Auranofin	provided by Dr. Spitz**	
Buthionine sulfoximine	Sigma, St. Louis, MO, USA	B2515
Decyl–triphenylphosphonium	provided by Dr. Spitz**	
Arsenic trioxide	Sigma, St. Louis, MO, USA	A1010
Dehydroepiandrosterone	Selleckchem, Houston, TX,USA	S2604
Rapamycin	LC Laboratories, Woburn, MA,USA	R–5000
Metformin	Sigma, St. Louis, MO, USA	PHR1084
Psychosine	Sigma, St. Louis, MO, USA	P9256
Balifomycin A1	Cayman, Ann Arbor, MI, USA	11038
Despramine	Sigma, St. Louis, MO, USA	D3900
Terfenadine	Sigma, St. Louis, MO, USA	T9652
Nutlin3	Selleckchem, Houston, TX,USA	S1061
KU55933	Selleckchem, Houston, TX,USA	S1092
NU7026	Selleckchem, Houston, TX,USA	S2839
SB202190	EMD Millipore, Billerica, MA, USA	559388
Parthenolide	Santa Cruz, Dallas, Texas, USA.	SC–3523
BMS345541	Sigma, St. Louis, MO, USA	B9935
JQ1	Cayman, Ann Arbor, MI, USA	11187
MG132	Sigma, St. Louis, MO, USA	M7449
IPI–504	Medchemexpress, Monmouth Junction, NJ, USA	HY–10210
Echinomycin	Cayman, Ann Arbor, MI, USA	11049
CPI–613	Selleckchem, Houston, TX,USA	S2776
Plumbagin	Sigma, St. Louis, MO, USA	P7262

Nature Medicine: doi:10.1038/nm.4010

Bortzomib	LC Laboratories, Woburn, MA,USA	B–1408
Wogonin	Cayman, Ann Arbor, MI, USA	14248
Phenethyl isothiocyanate (PEITC)	Sigma, St. Louis, MO, USA	253731
Spermine	Sigma, St. Louis, MO, USA	S3256
Trichostatin A (TSA)	Selleckchem, Houston, TX,USA	S1045
Vorinostat (SAHA)	Selleckchem, Houston, TX,USA	S1047
YM–155	Cayman, Ann Arbor, MI, USA	11490
Hydrogen peroxide	Fisher Scientific, Pittsburgh, PA, USA	H325
n–acetyl cysteine (NAC)	Sigma, St. Louis, MO, USA	a7250
MTT (3–(4,5–Dimethylthiazol–2–yl)–2,5–Diphenyltetrazolium Bromide) (MTT)	Sigma, St. Louis, MO, USA	M2128
Ganciclovir (GCV)	Sigma, St. Louis, MO, USA	G2536
Propidium iodide	Sigma, St. Louis, MO, USA	P4170
2–Mercaptoethanol	Sigma, St. Louis, MO, USA	M6250
Polyethylene glycol 400	Hampton Research, Aliso Viejo, CA, USA	HR2–603
Phosal 50 PG	American Lecithin Company, Oxford, CT, USA	368315–3130003/020
Collagenase, Type II	Thermo Fisher Scientific, Carlsbad, CA,USA	17101–015
Dispase II	Thermo Fisher Scientific, Carlsbad, CA,USA	17105–041
Collagen, Type I	Sigma, St. Louis, MO, USA	C3867
Mouse laminin protein	Thermo Fisher Scientific, Carlsbad, CA,USA	23017–015
Murine Stem Cell Factor (mSCF)	Peprotech, Rocky Hill, NJ, USA	250–03
Murine Fms–related tyrosine kinase 3 ligand (mFlt–3)	Peprotech, Rocky Hill, NJ, USA	250–31L
Murine Granulocyte Macrophage–Colony Stimulating Factor (mGM–CSF)	Peprotech, Rocky Hill, NJ, USA	315–03
Murine Interleukin–3 (mIL–3)	Peprotech, Rocky Hill, NJ, USA	213–13
Murine Thrombopoietin (mTPO)	Peprotech, Rocky Hill, NJ, USA	315–14
Murine Erythropoietin (mEPO)	R&D Systems, Minneapolis, MN, USA	959–ME–010
Murine Fibroblast Growth Factor–basic (bFGF)	Thermo Fisher Scientific, Carlsbad, CA,USA	PMG0033

*Dr. Nukhet Arkin–Burns, University of Arkansas for Medical Science

**Dr. Douglas Spitz, University of Iowa

Nature Medicine: doi:10.1038/nm.4010

Supplementary Table 3. Antibodies for western blot analyses

Antibody	Clone	Antibody isotype	Catalog #	Concentration
Bcl–2[1]	50E3	Rabbit IgG Monoclonal	2870S	1:1000
Bcl–xL[1]	_	Rabbit IgG Polyclonal	2762S	1:1000
Bak[1]	D4E4	Rabbit IgG Monoclonal	12105S	1:1000
Bax[1]	_	Rabbit IgG Polyclonal	2772S	1:1000
Mcl–1[1]	D35A5	Rabbit IgG Monoclonal	5453S	1:1000
Bim[1]	C34C5	Rabbit IgG Monoclonal	2933S	1:500
Caspase–3[1]	_	Rabbit IgG Polyclonal	9662S	1:1000
Cleaved Caspase–3[1]	_	Rabbit IgG Polyclonal	9661S	1:1000
Caspase–8[1]	1C12	Rabbit IgG Monoclonal	9746S	1:1000
RIP1[1]	D94C12	Rabbit IgG Monoclonal	3493S	1:1000
Bid[2]	_	Rabbit IgG Polyclonal	SC–11423	1:200
β–actin[2]	_	Goat IgG Polyclonal	SC–1615	1:1000
Bad[3]	48/Bad	Mouse IgG2b	610391	1:500
Noxa[4]	114C307	Mouse IgG Monoclonal	OP180	1:500

Footnotes: [1] Cell signaling, Danvers, MA, USA; [2]Santa Cruz, Dallas, Texas, USA; [3]BD Biosciences, San Jose, CA, USA; [4]EMD Millipore Corporation, San Diego, CA, USA.

Nature Medicine: doi:10.1038/nm.4010

Supplementary Table 4. Antibodies for flow cytometry and cell sorting

Antibody	Clone	Antibody	Conjugate	Concentration
CD45R / B220[1]	RA3–6B2	IgG_{2a}	purified	1:200
CD3e[1]	145–2C11	IgG_1	purified	1:200
CD11b[1]	M1/70	IgG_{2b}	purified	1:200
Gr–1[1]	RB6–8C5	IgG_{2b}	purified	1:200
Ter–119[1]	Ter–119	IgG_{2b}	purified	1:200
CD45R / B220[1]	RA3–6B2	IgG_{2a}	biotin	1:200
CD3e[1]	145–2C11	IgG_1	biotin	1:200
CD11b[1]	M1 / 70	IgG_{2b}	biotin	1:200
Gr–1[1]	RB6–8C5	IgG_{2b}	biotin	1:200
Ter–119[1]	Ter–119	IgG_{2b}	biotin	1:200
CD16 / CD32[1]	2.4G2	IgG_{2b}	Purified	1:200
CD45.2[1]	104	IgG_{2a}	FITC	1:100
CD45R / B220[1]	RA3–6B2	IgG_{2a}	APC	1:200
CD45R / B220[1]	RA3–6B2	IgG_{2a}	PE	1:200
CD90.2[1]	53–2.1	IgG_{2a}	APC	1:200
CD11b[1]	M1 / 70	IgG_{2a}	PE	1:200
Gr–1[1]	RB6–8C5	IgG_{2a}	PE	1:200
Streptavidin	Streptavidin		FITC	1:200
Sca1[1]	E13–161.7	IgG_{2a}	PE	1:100
Sca1[1]	E13–161.7	IgG_{2a}	PE–Cy™ 7	1:100
CD135[1]	4G8	IgG_1	PE	1:100
c–kit[1]	2B8	IgG_{2b}	APC–H7	1:100
c–kit[2]	2B8	IgG_{2b}	APC–eFluor® 780	1:100
CD150[2]	9D1	IgG_{2a}	APC	1:100
CD34[2]	RAM34	IgG_{2a}	Alexa Fluor® 700	1:20
Ki–67[2]	20Raj1	IgG_1	FITC	1:50
Ki–67[2]	20Raj1	IgG_1	Alexa Fluor® 700	1:50

CD48[3]	HM481	IgG_{2a}	Pacific blue	1:200
γH2AX[3]	2F3	IgG_1	FITC	1:200
CD93[2]	AA4.1	IgG_{2b}	PE–Cy7	1:100
IgM[2]	II/41	IgG_{2a}	APC	1:100
p–p38[4]	28B10	IgG_1	Alexa Fluor® 488	1:100
CD45[1]	30–F11	IgG_{2b}	APC	1:200
CD11b[1]	M1 / 70	IgG_{2b}	APC	1:200
Sca–1[2]	D7	IgG_{2a}	Alexa Fluor® 700	1:200
CXCR4[3]	L276F12	IgG_{2b}	PE	1:50
Integrin β1[3]	HMβ1–1	IgG	Pacific blue	1:800
P16[5]	F–12	IgG_{2a}	purified	1:100
γH2AX[6]	JBW301	IgG_1	purified	1:1000
Pax7[8]	—	MIgG1, kappa	purified	1:20
Goat Anti–Mouse IgG (H+L)[7]	—	IgG (H+L)	Alexa Fluor® 488	1:1000

Footnotes: [1]BD Biosciences, San Jose, CA; [2]eBioscience, San Jose, CA; [3]Biolegend, San Diego, CA; [4]Cell Signaling, Danvers, MA, USA; [5]Santa Cruz Biotechnology, Dallas, TX, USA; [6]EMD Millipore Corporation, San Diego, CA, USA; [7]Thermo Fisher Scientific, Carlsbad, CA, USA; [8]Developmental Studies Hybridoma Bank, Iowa City, IA, USA.

Nature Medicine: doi:10.1038/nm.4010

Supplementary Table 5. Sequences of the primers used for qRT–PCR

Gene	Forward sequences	Reverse sequences
Human *CDKN2A*[1]	5–CCAACGCACCGAATAGTTACG–3	5–GCGCTGCCCATCATCATG–3
Human *CDKN1A*[2]	5–GACAGCAGAGGAAGACCATGTGGAC–3	5–GAGTGGTAGAAATCTGTCATGCTG–3
Human *GAPDH*[1]	Cat# 4331182	Cat# 4331182
Mouse *Cdkn2a*[1]	5–CGGTCGTACCCCGATTCAG–3	5–GCACCGTAGTTGAGCAGAAGAG–3
Mouse *Hprt*[1]	Cat# 4351370	Cat# 4351370
Mouse *Il1a*[2]	5–CCATAACCCATGATCTGGAAGAGAC–3	5–GTCCACATCCTGATATATAGTTTG–3
Mouse *Il1b*[2]	5–CCATAACCCATGATCTGGAAGAGAC–3	5–GTCCACATCCTGATATATAGTTTG–3
Mouse *Il6*[2]	5–CTGCAAGAGACTTCCATCCAG–3	5–AGTGGTATAGACAGGTCTGTTGG–3
Mouse *Tgfb1*[2]	5–CCACGTGGAAATCAACGGGATCAG–3	5–GTGCCGTGAGCTGTGCAGGTGCTG–3
Mouse *Tnfa*[2]	5–TGAACTTCGGGGTGATCGGTC–3	5–CACTTGGTGGTTTGCTACGACG–3
Mouse *Ccl5*[2]	5–CCCGCACCTGCCTCACCATATGG–3	5–CCTTCGAGTGACAAACACGACTG–3
Mouse *Cxcl10*[2]	5–GGTCTGAGTGGGACTCAAGGGATC–3	5–TCATCGTGGCAATGATCTCAACAC–3
Mouse *Hprt*[2]	5–AGCAGTACAGCCCCAAAATGGTTA–3	5–TCAAGGGCATATCCAACAACAAAC–3

Footnotes: [1]Life technologies, Grand Island, NY, USA; [2]Integrated DNA Technologies, Coralville, IA, USA